Dual-Surface Modified Virus Capsids for Targeted Delivery of Photodynamic Agents to Cancer Cells

Nicholas Stephanopoulos, Gary J. Tong, Sonny C. Hsiao, and Matthew B. Francis*

Department of Chemistry, University of California, Berkeley, and Materials Sciences Division, Lawrence Berkeley National Laboratories, Berkeley, California 94720-1460

ABSTRACT Bacteriophage MS2 was used to construct a targeted, multivalent photodynamic therapy vehicle for the treatment of Jurkat leukemia T cells. The self-assembling spherical virus capsid was modified on the interior surface with up to 180 porphyrins capable of generating cytotoxic singlet oxygen upon illumination. The exterior of the capsid was modified with ~20 copies of a Jurkat-specific aptamer using an oxidative coupling reaction targeting an unnatural amino acid. The capsids were able to target and selectively kill more than 76% of the Jurkat cells after only 20 min of illumination. Capsids modified with a control DNA strand did not target Jurkat cells, and capsids modified with the aptamer were found to be specific for Jurkat cells over U266 cells (a control B cell line). The doubly modified capsids were also able to kill Jurkat cells selectively even when mixed with erythrocytes, suggesting the possibility of using our system to target blood-borne cancers or other pathogens in the blood supply.

KEYWORDS: viral capsids · photodynamic therapy · porphyrins · aptamers · targeted delivery

M uch recent attention has been devoted to the development of nanoscale delivery agents for use in tissue-targeted therapy and diagnostic imaging.[1-5] Relative to small molecules, nanoscale carriers offer prolonged circulation times and selective access to cancer tissue through the enhanced permeation and retention effect.[6] Even more importantly, the relatively large size of these objects allows them to house a significantly increased drug payload and to achieve higher targeting specificity through multivalency effects.[7-9] A variety of approaches have been advanced toward this end, including the use of polymers,[10-12] dendrimers,[13-16] inorganic nanoparticles,[17-19] and liposomes.[20,21] Chemically modified viral capsids have provided another platform for these studies,[22] as they offer uniform sizes and the opportunity to attach multiple functional groups to their internal and external surfaces through appropriately designed chemical strategies. As an added advantage, the multiple protein subunits comprising their shells will ultimately be

dissociated and degraded, thus avoiding undesired bioaccumulation. Because of these promising features, a number of laboratories are working to develop new carriers based on these assemblies.

We recently reported[23,24] the construction of a targeted multivalent delivery vehicle using the protein shell of bacteriophage MS2, a 27 nm spherical virus comprising 180 identical protein monomers.[25] The individual proteins can be produced recombinantly in *E. coli*, which results in their spontaneous assembly into hollow protein shells that are free of genomic material. A uniquely reactive cysteine residue (C87) was introduced into the sequence of each monomer to allow facile modification of the capsid interior with maleimide reagents, Figure 1.[23] To functionalize the outside surface with targeting molecules of varying composition, we used the amber codon suppression method developed by the Schultz lab[26,27] to introduce the unnatural amino acid *p*-aminophenylalanine[28] (*p*aF). The aniline groups of these side chains can be modified with *N,N*-dialkylphenylene diamine derivatives through a highly chemoselective oxidative coupling strategy.[29]
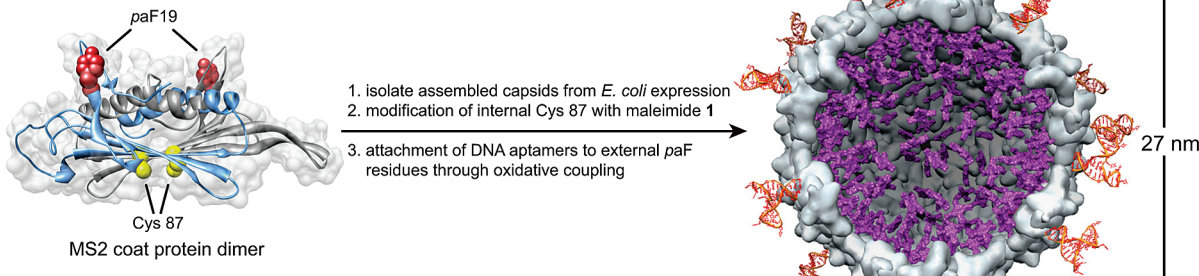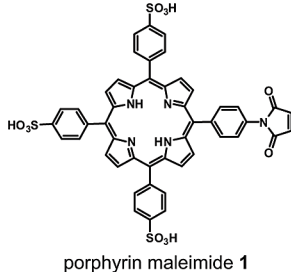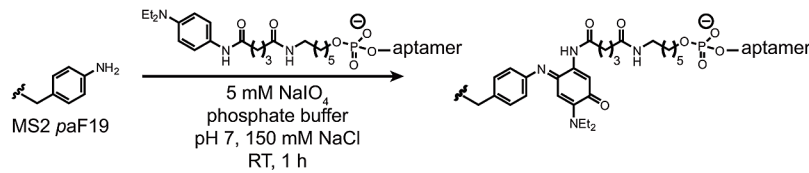
Although many biomolecule types can be added to viral capsids to endow them with targeting capabilities, DNA aptamers[30-39] provide a particularly attractive and convenient option. They are well-defined, easily synthesized, and can be evolved to recognize a wide variety of epitopes using the SELEX procedure.[40-42] DNA aptamers are more stable than their RNA counterparts *in vivo*, and studies have shown that backbone substitutions can be used to enhance this stability further.[43,44] We have previously shown[23] that multiple

*Address correspondence to
francis@cchem.berkeley.edu.

Figure 1. Construction of a multivalent cell-targeted photodynamic therapy vehicle using recombinant bacteriophage MS2. Cysteine residues on the capsid interior were modified using porphyrin maleimide **1** (rendered in purple), enabling the generation of singlet oxygen upon illumination at 415 nm. Exterior *p*-aminophenylalanine (*p*aF) residues introduced using the Schultz amber suppression technique[26−28] were coupled to phenylene diamine modified DNA aptamers previously shown[23] to bind tyrosine kinase 7 receptors. About 20 aptamers were installed on each capsid surface. The orange DNA strands in the cartoon are based on a structurally characterized DNA aptamer of different sequence, but similar length (PDB ID: 3HXO).[43] They are included only to portray the relative sizes of the biomolecular components.
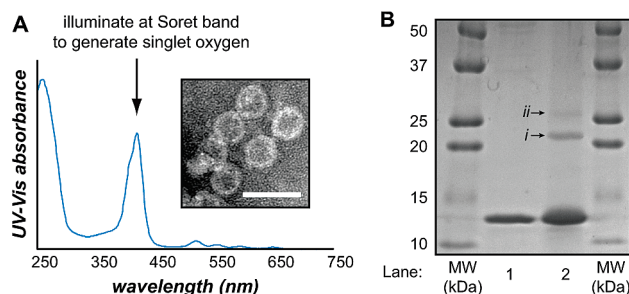
copies of an aptamer targeting protein tyrosine kinase 7 (PTK7) receptors on Jurkat leukemia T cells (strand **A**, reported by the Tan lab as sgc8c[45−47]) can be attached to MS2 capsids to achieve efficient and selective cell targeting. In our initial studies, fluorescent cargo was installed to allow tracking of the capsids following endocytosis.[23] The next step in these studies is the attachment of drug molecules in order to treat the cells that have been targeted.

Photodynamic therapy (PDT) involves the generation of singlet oxygen molecules by a sensitizing group.[48,49] Porphyrins are commonly used for this purpose because they have high extinction coefficients and exhibit efficient intersystem crossing to the triplet state.[50,51] The singlet oxygen they produce is highly reactive, and leads to nonspecific damage to the cell membranes. This results in both necrotic and apoptotic cell death, depending on the location at which the damage occurs. Viral capsids have indeed been used to deliver iodoacetamide modified Ru(bpy)$_2$(phen)$^{3+}$ complexes to *Staphylococcus aureus* bacteria by virtue of electrostatics and biotinylated antibodies.[52] These studies highlighted the advantages of using a macromolecular scaffold to deliver multiple copies of the sensitizers for more efficient oxygen generation. In addition, a recent report utilized aptamer−porphyrin conjugates for photodynamic therapy,[53] but the advantages of viral capsids and aptamers have yet to be combined for PDT.

RESULTS AND DISCUSSION

We sought to employ our aptamer-modified capsids for a photodynamic treatment for Jurkat T cells by replacing the fluorescent dye used in our initial report with a porphyrin that would generate singlet oxygen upon illumination. By placing the cargo inside the capsids, the overall impact on the solubility and nonspecific interactions of the particles was expected to be minimized. Previous approaches toward the photodynamic therapy of Jurkat cells have been reported using porphyrins, phthalocyanines, and other dyes.[54−56] To convert MS2 capsids into targeted sensitizers, we synthesized porphyrin maleimide **1** according to literature protocols.[57−59] Upon exposure of N87C MS2 capsids to this reagent at pH 7 for 2 h, virtually 100% of the capsid monomers were modified, as determined by UV−vis analysis (see Supporting Information for characterization details), installing up to 180 porphyrins on the inside surface of the virus. Reversed-phase HPLC analysis confirmed the high level of conversion and indicated that free porphyrin was not associating with the capsids through nonspecific interactions. Exposure of maleimide **1** to MS2 capsids lacking C87 did not lead to protein modification.

We next attached *N,N*-diethylphenylene diamine-substituted DNA aptamer **A** to the *p*aF group on the exterior of the capsid using sodium periodate, as previously described.[23] This procedure resulted in the installation of about 20 copies of the 41-nt aptamer on

Figure 2. Characterization of porphyrin-containing MS2 capsids with aptamer targeting groups. (A) The UV−vis spectrum of the MS2-1-A conjugate clearly shows the Soret absorbance of the porphyrin, which can be illuminated to generate singlet oxygen. Inset: TEM image of MS2-1-A sample, indicating that the capsids are still intact after the dual surface modification (scale bar: 50 nm). (B) Gel analysis of the MS2-1-A double conjugate shows a new band (i) corresponding to the attachment of the aptamer. A very small amount of capsid protein dimer (ii) is also observed, corresponding to reaction between adjacent *p*aF residues on the capsid surface. Lane 1: wtMS2. Lane 2: MS2-1-A.

each capsid, as determined by an SDS-PAGE gel shift (Figure 2B). Although higher conversion can likely be obtained under more rigorous conditions, the addition of this much DNA already provides a net change in charge of −800 on each particle, and provides enough aptamer strands to achieve cell targeting. The capsids remained spherical and intact throughout the dual-surface modification procedure, as evidenced by size-exclusion chromatography (SEC) and transmission electron microscopy (see Figure 2A inset and Supporting Information Figures S3 and S4).
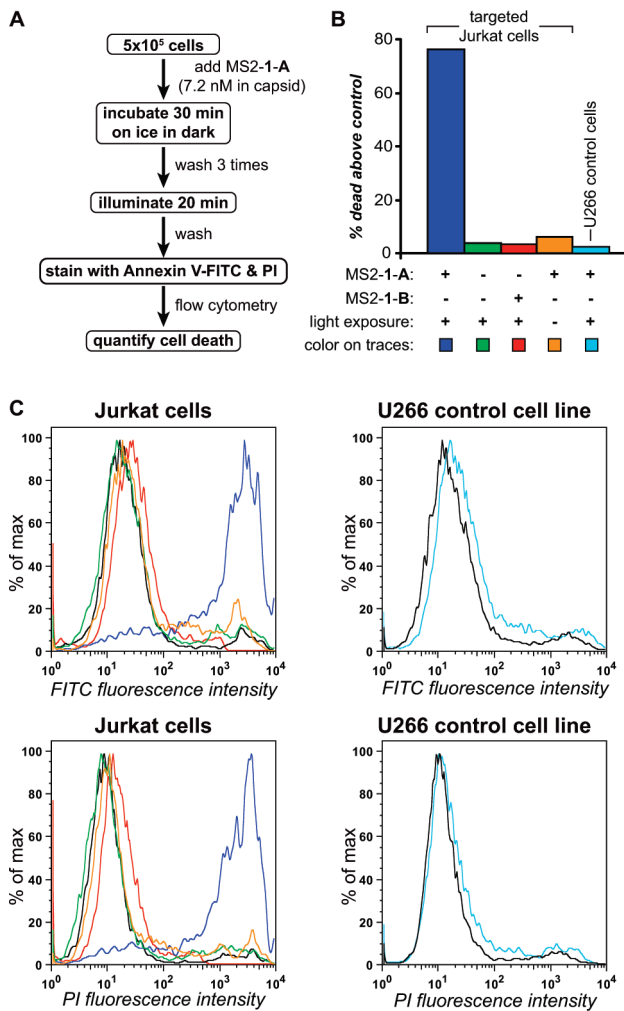
After dual-surface modification, we wanted to confirm the ability of the capsids to produce singlet oxygen upon illumination. We used anthracene-9,10-dipropionic acid (ADPA) as a detector (see Supporting Information for details), as it is known to undergo a rapid cycloaddition reaction with singlet oxygen molecules.[60] Loss of ADPA was quantified using HPLC and UV−vis analysis of the ADPA solution after 20 min of illumination with a 415 nm LED lamp targeting the porphyrin's Soret absorption band (Figure 2A). Using this ADPA assay, we determined that each capsid produced at least 360 000 molecules of singlet oxygen (2000 molecules/porphyrin) in this time frame. As a certain fraction of the singlet oxygen was likely not captured by the indicator, this value represents a lower estimate. Remarkably, SEC analysis of the resulting sample indicated that the capsids were both still largely intact (Supporting Information Figure S3), and that both the porphyrin and the aptamer remained attached, a fact further verified by SDS-PAGE. Thus, the carriers could be used to generate singlet oxygen for longer times, should applications require them. Illumination was necessary for singlet oxygen production, and illumination of aptamer-modified MS2 capsids that lacked the internal porphyrin groups did not lead to any detectable consumption of the ADPA indicator during the same time period.

To determine the photodynamic efficiency and specificity of the capsids toward receptor-positive cells,

we labeled N87C *p*aF19 MS2 capsids with porphyrin **1** and either Jurkat-specific aptamer **A** or a 41-nt control strand **B** (which does not bind Jurkat cells[23]). As a negative control, we used U266 cells, which are a B lymphocyte cell line that was previously reported not to bind aptamer **A**.[45] We then exposed 5×10^5 cells of either type to solutions of 7.2 nM (in capsid) MS2-1-A and incubated the mixtures for 30 min on ice in the dark. Next, the cells were washed to remove any unbound capsids and illuminated for 20 min using a 415 nm LED lamp to generate singlet oxygen. This protocol is summarized in Figure 3A.

Following illumination, cell viability was assayed by staining with Annexin V-FITC (which detects apoptosis) and propidium iodide (PI, which detects compromised cell membranes, due to either necrosis or late-stage apoptosis).[61] The samples were then analyzed using flow cytometry, Figure 3C. Jurkat cells exposed to MS2-1-A and 415 nm illumination showed a dramatic increase (over 100-fold) in both Annexin V-FITC and PI fluorescence over untreated Jurkat cells, demonstrating the photodynamic efficiency of the capsids. By comparison, Jurkat cells treated with MS2-1-A but kept in the dark, Jurkat cells illuminated in the absence of MS2-1-A, and Jurkat cells illuminated after treatment with MS2-1-B did not show any significant increase in either Annexin V-FITC or PI staining compared to untreated cells. Additionally, U266 cells exposed to the same concentration of MS2-1-A and illuminated for 20 min also showed no significant increase in either stain's fluorescence, demonstrating the potential for the aptamers to target one cell type selectively. The Annexin V-FITC and PI staining results were used to determine the amount of cell death relative to a control sample of untreated cells. Over 76% of Jurkat cells illuminated in the presence of MS2-1-A were dead (relative to an untreated control), whereas a much smaller percentage (3−6%) of cells had died in the control samples, Figure 3B. This value of 76% represents a lower limit; due to the damage caused by the singlet oxygen to cell membranes, we were not able to recover nearly as many cells for flow cytometry analysis with the MS2-1-A samples as with the control samples, so it is likely that the percentage killed is actually much higher.

It was important to tune the amount of MS2-1-A added (7.2 nM in capsid). Decreasing the amount of capsid by a factor of 2 resulted in a noticeably lower amount of cell death, presumably because less singlet oxygen was generated overall. Doubling the capsid concentration, however, resulted in a greater amount of death in Jurkat cells treated with an equivalent amount of MS2-1-B, most likely due to nonspecific association of the capsids with cells at higher concentrations. An illumination time of 20 min was chosen in order to have the greatest amount of cell death in the smallest amount of time, thus maximizing the effectiveness of the treatment; increasing the time resulted in a greater degree of death

A

B

C

Figure 3. Flow cytometry analysis of the photodynamic cell killing efficiency of modified MS2 capsids. The experimental procedure is outlined in panel A. Illumination was at 415 nm for 20 min. The obtained flow cytometry data are summarized in panel B, and raw traces are provided in panel C. Aptamer sequence **A** targeted PTK7 on Jurkat cell surfaces, while sequence **B** was a nontargeted control. The black traces correspond to untreated cell samples. Significant cell death was only observed for Jurkat cells and only upon treatment with MS2-**1-A** and light. Samples were analyzed after staining with Annexin V-FITC (top traces) and propidium iodide (PI, bottom traces).
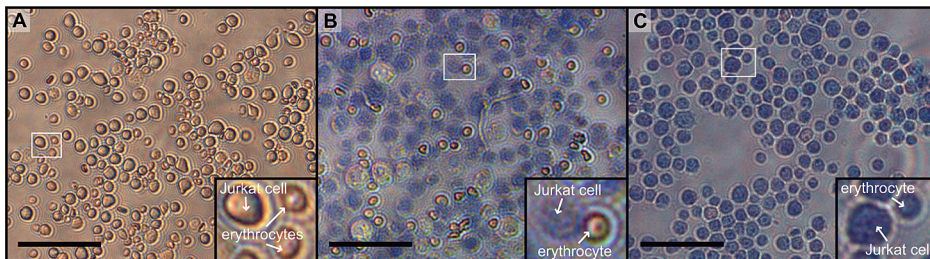
the situation at hand, as is required for the development of a proper dosing regimen for all drugs.

One of the traditional limitations of photodynamic therapy using porphyrins is the shallow penetration depth of the blue light used to excite them at their absorbance maximum.[48] The Q-bands can be excited at longer wavelengths, but with reduced efficiency due to the markedly lower extinction coefficients. As Jurkat cells are a carcinogenic T cell line that circulates in the blood, however, it could be possible to expose them to light using a continuous dialysis system in which a bypass would be used to remove blood from a patient. This approach would circumvent the issue of penetration depth and allow for the photodynamic therapy of blood-borne cancers. With alternative targeting strategies, this system could also be used to kill other pathogens that are present in the circulatory system or in the blood supply.

To test the feasibility of this approach, we sought to determine whether we could selectively target Jurkat cells in the presence of red blood cells. Because singlet oxygen has a diffusion length of ~100 nm,[62] capsids bound to or internalized by Jurkat cells should be able to damage the T cells without affecting nearby blood cells. We first modified the cell surfaces of a mixed population of erythrocytes and Jurkat cells with single-stranded DNA using an NHS-ester based technique developed in our lab.[63] We immobilized this mixture of cells on a glass slide bearing the complementary DNA strand, resulting in a heterogeneous population of the two cell types, Figure 4A. Jurkat cells are noticeably larger than erythrocytes and have a different morphology, allowing them to be distinguished readily through simple visual inspection.

We then applied a solution of 7.2 nM (in capsid) MS2-**1-A** to the slide, incubated it for 30 min on ice in the dark, and washed the cells to remove unbound capsids. The cells were then illumi-

for untargeted samples. Thus, the amount of applied capsid and the illumination time must be adjusted for


Figure 4. Selective killing of Jurkat T cells in the presence of erythrocytes. Cell populations were combined and attached to glass slides through DNA-based adhesion, as described in the text. After exposure to the experimental conditions, all samples were exposed to trypan blue (which stains dead cells) and then rinsed with PBS. (A) Live control cells. The Jurkat cells can be distinguished from the red blood cells based on size and shape. (B) Cells exposed to 7.2 nM MS2-**1-A** capsids at 0 °C, and then irradiated with 415 nm light for 20 min at room temperature. Only the larger Jurkat cells are dead, as indicated by the trypan blue stain. The smaller red blood cells are unharmed. (C) Positive control cells exposed to 30% EtOH before staining to induce cell death. Both Jurkat and red blood cells stain equally well with trypan blue. Scale bars: 100 μm.

nated for 20 min at 415 nm and assayed for cell viability. Based on the PI staining results in Figure 3, we expected the singlet oxygen to cause widespread necrosis due to membrane damage. However, we could not use the PI stain to assay the red blood cells because they lack the genomic DNA to which the stain binds. Instead, we used trypan blue, a dye that stains cells that have compromised membranes.[64] Figure 4 shows the bright-field microscope images of the immobilized mixture of red blood and Jurkat cells before (Figure 4A) and after (Figure 4B) treatment with MS2-**1**-**A** and illumination. Before treatment, none of the cells have taken up the trypan blue stain, indicating viability of both the erythrocytes and the Jurkat cells. Roughly 38% of the cells in Figure 4A were red blood cells, as determined by their size and shape.

After treatment, the majority of the Jurkat cells stained positive for cell death, and the majority of the remaining unstained cells were red blood cells. The live erythrocytes corresponded to 33% of the total cells in Figure 4B, indicating that only a small fraction (~5%) of the cells were dead red blood cells. By contrast, live Jurkat cells comprised only 9% of the total cells in Figure 4B, further validating the effectiveness of the treatment. Even red blood cells directly adjacent to a dead Jurkat cell remained viable (Figure 4B, inset), confirming that the therapeutic range of the singlet oxygen was closely limited to the targeted cells. We also performed a positive control where we killed the mixed population of cells with 30% EtOH in order to confirm that the red blood cells stained as readily as the Jurkat cells (Figure 4C).

These studies indicate the promise of using dual-modified viral capsids as targeted therapeutic vehicles.

In principle, aptamers can be evolved to bind almost any cellular target, lending a wide degree of flexibility to this approach. Furthermore, the oxidative coupling strategy used can be extended to a variety of other targeting epitopes such as peptides or antibody fragments. Because the penetration depth of 415 nm light in tissue is quite limited, this porphyrin-based method will be limited to use in surface cancers or in blood samples. However, efforts are underway to replace the cargo inside the capsids with phthalocyanines, which can generate singlet oxygen upon illumination at their peak absorbance in the near-infrared region of the spectrum. This should allow for efficient treatment with significantly better tissue penetration.

SUMMARY

We have used bacteriophage MS2 to create a targeted, multivalent photodynamic therapy vehicle for Jurkat leukemia T cells. By modifying the interior surface with porphyrins capable of generating large amounts of singlet oxygen upon illumination and the outside of the capsid with cell receptor-specific DNA aptamers, we were able to target and kill significant numbers of cells in only 20 min. The targeting was specific for the Jurkat cells, with U266 B lymphocytes not being affected by the treatment. Furthermore, the dual-functionalized capsids were able to target and kill Jurkat cells selectively when mixed with erythrocytes due to the short diffusion length of singlet oxygen. This multivalent sytem has the advantage of modularity, allowing the attachment of any maleimide drug on the inside and any evolved aptamer on the outside. It can therefore be adapted readily to deliver cargo to a wide variety of cellular targets.

METHODS

Production of N87C T19paF MS2. The unnatural amino acid *p*-aminophenylananine (*p*aF) was incorporated into MS2 as previously described.[28] The N87C/T19*p*aF mutant plasmid was created by site-directed mutagenesis of the pBAD-T19*p*aF MS2 vector following the Qiagen protocol with forward primer 5′-AGCCGCATGGCGTTCGTACTTATGTATGGAACTAACCA TTC-3′ and reverse primer 5′-GAATGGTTAGTTCCATACATAAG TACGAACGCCATGCGGCT-3′. The pBAD-N87C/T19*p*aF was subsequently grown and purified as previously described.[28]

Modification of MS2 with Porphyrin 1. To a solution of N87C T19*p*aF MS2 (80 μM) in 10 mM phosphate buffer, pH 7) was added 20 equiv of porphyrin maleimide **1** as a 50 mM solution in DMSO. The reaction mixture was vortexed briefly, then incubated at room temperature (RT) for 2 h in the dark. The mixture was then passed through a NAP-5 column equilibrated with 10 mM phosphate buffer, pH 7, to remove excess porphyrin. The capsids were further concentrated using a 100 kDa molecular weight cutoff filter. The conversion of porphyrin was determined by comparing the absorbance of the porphyrin Soret band ($\varepsilon = 266\,000$ M^{-1} cm^{-1}) to the A260 of the protein ($\varepsilon = 172\,000$ M^{-1} cm^{-1}) and assuming negligible porphyrin absorbance at 260 nm.

DNA Attachment *via* Oxidative Coupling. Strands **A** and **B** were attached to capsids modified with porphyrin **1** as previously described.[23] To synthesize the phenylene diamine conjugate necessary for the oxidative coupling, DNA strands containing a primary amine at the 5′-end were reacted with 4-(4-diethylamino-phenylcarbamoyl)-butyric acid (60−120 equiv) in a 1:1 solution of DMF and 50 mM phosphate buffer, pH 8. The reaction mixture was allowed to react at RT for 2 h, then purified by gel filtration to remove excess small molecules. The DNA was lyophilized and resuspended in the desired buffer. The concentration was determined by the absorbance at 260 nm.

The phenylene diamine-modified DNA was next attached to the MS2-**1** capsids *via* the oxidative coupling reaction as previously described.[23] An Eppendorf tube was charged with MS2-**1** (20 μM), the phenylene diamine-modified oligonucleotide (200 μM), and NaIO₄ (5 mM). The reaction mixture was vortexed and allowed to react at RT for 1 h. The reaction was quenched by the addition of 1/10 volume of 500 mM *tris*-(2-carboxyethyl)phosphine (TCEP), pH 7, then purified by NAP-5 filtration and spin-concentration. The sequences of the strands are as follows: strand **A**, 5′-ATCTAACTGCTGCGCCGCCGGGAA-AATACTGTACGG TTAGA-3′; strand **B**, 5′-CCCTAGAGTGAG-TCGTATGACCCTA GAGTGAGTCGTATGAA-3′.

Flow Cytometry Experiments. To quantify cell death, we used flow cytometry to analyze the annexin V-FITC and PI staining intensities of the treated samples. For all experiments, we used 5 × 105 cells (either Jurkat or U266) suspended in 1 mL of PBS containing 1% FBS. To these cells was added 200 μL of MS2-**1**-**A** (or MS2-**1**-**B**) at a concentration of 1.3 μM in protein monomer, or 7.2 nM in capsid (roughly 1.75 × 106 capsids/cell). The cells were

incubated with the capsids for 30 min on ice in the dark, then washed three times by centrifugation (240 g) followed by resuspension in 1 mL of PBS containing 1% FBS. They were then placed in glass-bottomed wells and illuminated for 20 min using a 415 nm LED lamp.

Following illumination, the cells were washed once by centrifugation, resuspended in the apoptosis kit binding buffer, and stained with annexin-V FITC and PI. Following staining, the cells were analyzed by flow cytometry to determine the amount of FITC and PI fluorescence. To determine the amount of cell death in Figure 3B, the flow cytometry results were gated using a control sample of live, healthy cells that had not been treated with anything. For each experiment, a population of cells not exposed to any treatment was also used to control for variability in cell viability from day to day.

For the flow cytometry results, 10 000 cells were counted when possible. However, for the cells treated with MS2-**1**-**A** and light, many cells were lost after the illumination step, presumably because the membrane damage caused by singlet oxygen prevented them from forming a pellet upon centrifugation. As a result, only 3000 cells were counted for this sample.

Photodynamic Treatment of Jukat Cells in a Surface-Immobilized Mixed Jurkat-Erythrocyte Population. A mixed population of Jurkat cells and erythrocytes was immobilized on a glass slide as previously described.[63] Briefly, fresh samples of red blood cells were obtained from a blood sample of a healthy human and stored in a 1% citric acid solution at room temperature. Cells were used within 1 h. Both Jurkat cells and erythrocytes were exposed to the same sample of single-stranded DNA modified with an NHS ester in order to attach DNA on the cell surface proteins. This mixed population was then immobilized on a glass slide bearing the cDNA sequence. Because both cell types were modified with the same DNA strand, the immobilized population was heterogeneous.

Next, the surface-immobilized cells were exposed to 200 μL of a solution of MS2-**1**-**A** (7.2 nM in capsid) for 30 min, on ice in the dark. The slides were rinsed with three portions of 1 mL of PBS containing 1% FBS and then illuminated with a 415 nm lamp for 20 min. Following illumination, cell viability was assayed using trypan blue to detect cell death. A negative control slide, consisting of mixed cells not exposed to capsids, was also stained by trypan blue to show cell viability. Finally, a positive control slide, consisting of mixed cells exposed to 30% ethanol, demonstrated that both cell types stained blue upon death.

Supporting Information Available: Full characterization of conjugates, quantification of singlet oxygen production, and additional Jurkat targeting experiments are provided. This material is available free of charge *via* the Internet at http://pubs.acs.org.

REFERENCES AND NOTES

1. Delehanty, J. B.; Boeneman, K; Bradburne, C. E.; Robertson, K.; Medintz, I. L. Quantum Dots: A Powerful Tool for Understanding the Intricacies of Nanoparticle-Mediated Drug Delivery. *Expert Opin. Drug Delivery* **2009**, *6*, 1091–1112.

2. Lammers, T.; Hennink, W. E.; Storm, G. Tumour-Targeted Nanomedicines: Principles and Practice. *Br. J. Cancer* **2008**, *99*, 392–397.

3. Cai, W.; Chen, X. Nanoplatforms for Targeted Molecular Imaging in Living Subjects. *Small* **2007**, *3*, 1840–1854.

4. Aubin-Tam, M. E.; Hamad-Schifferli, K. Structure and Function of Nanoparticle-Protein Conjugates. *Biomed. Mater.* **2008**, *3*, 034001.

5. Brannon-Peppas, L.; Blanchette, J. O. Nanoparticle and Targeted Systems for Cancer Therapy. *Adv. Drug Delivery Rev.* **2004**, *56*, 1649–1659.

6. Maeda, H.; Wu, J.; Sawa, T.; Matsumura, Y.; Hori, K. Tumor Vascular Permeability and the EPR Effect in Macromolecular Therapeutics: A Review. *J. Controlled Release* **2000**, *65*, 271–284.

7. Lu, Y. J.; Low, P. S. Folate-Mediated Delivery of Macromolecular Anticancer Therapeutic Agents. *Adv. Drug Delivery Rev.* **2002**, *54*, 675–693.

8. Kiessling, L. L.; Gestwicki, J. E.; Strong, L. E. Synthetic Multivalent Ligands as Probes of Signal Transduction. *Angew. Chem., Int. Ed.* **2006**, *45*, 2348–2368.

9. Mammen, M.; Choi, S. K.; Whitesides, G. M. Polyvalent Interactions in Biological Systems: Implications for Design and Use of Multivalent Ligands and Inhibitors. *Angew. Chem., Int. Ed.* **1998**, *37*, 2754–2794.

10. Liu, S.; Maheshwari, R.; Kiick, K. L. Polymer-Based Therapeutics. *Macromolecules* **2009**, *42*, 3–13.

11. Farokhzad, O. C.; Cheng, J.; Teply, B. A.; Sherifi, I.; Jon, S.; Kantoff, P. W.; Richie, J. P.; Langer, R. Targeted Nanoparticle—Aptamer Bioconjugates for Cancer Chemotherapy *in Vivo*. *Proc. Natl. Acad. Sci., U.S.A.* **2006**, *103*, 6315–6320.

12. Dhar, S.; Gu, F. X.; Langer, R.; Farokhzad, O. C.; Lippard, S. J. Targeted Delivery of Cisplatin to Prostate Cancer Cells by Aptamer Functionalized Pt(IV) Prodrug-PLGA-PEG Nanoparticles. *Proc. Natl. Acad. Sci., U.S.A.* **2008**, *105*, 17356–17361.

13. Ihre, H. R.; Padilla De Jesús, O. L.; Szoka, F. C., Jr.; Fréchet, J. M. J. Polyester Dendritic Systems for Drug Delivery Applications: Design, Synthesis, and Characterization. *Bioconjugate Chem.* **2002**, *13*, 443–452.

14. Padilla De Jesús, O. L.; Ihre, H. R.; Gagne, L.; Fréchet, J. M. J.; Szoka, F. C. Polyester Dendritic Systems for Drug Delivery Applications: *In Vitro* and *in Vivo* Evaluation. *Bioconjugate Chem.* **2002**, *13*, 453–461.

15. Gillies, E. R.; Fréchet, J. M. J. Designing Macromolecules for Therapeutic Applications: Polyester DendrimerPoly(ethylene oxide) "Bow-Tie" Hybrids with Tunable Molecular Weight and Architecture. *J. Am. Chem. Soc.* **2002**, *124*, 14137–14146.

16. Wolinsky, J. B.; Grinstaff, M. W. Therapeutic and Diagnostic Applications of Dendrimers for Cancer Treatment. *Adv. Drug Delivery. Rev.* **2008**, *60*, 1037–1055.

17. Liong, M.; Lu, J.; Kovochich, M.; Xia, T.; Ruehm, S. G.; Nel, A.; Tamanoi, F.; Zink, J. I. Multifunctional Inorganic Nanoparticles for Imaging, Targeting, and Drug Delivery. *ACS Nano* **2008**, *2*, 889–896.

18. Medarova, Z.; Pham, W.; Farrar, C.; Petkova, V.; Moore, A. *In Vivo* Imaging of siRNA Delivery and Silencing in Tumors. *Nat. Med.* **2007**, *13*, 372–377.

19. Javier, D. J.; Nitin, N.; Levy, M.; Ellington, A.; Richards-Kortum, R. Aptamer-Targeted Gold Nanoparticles as Molecular-Specific Contrast Agents for Reflectance Imaging. *Bioconjugate Chem.* **2008**, *19*, 1309–1312.

20. Lee, R.; Low, P. J. Delivery of Liposomes into Cultured KB Cells *via* Folate Receptor-Mediated Endocytosis. *J. Biol. Chem.* **1994**, *269*, 3198–3204.

21. Medinai, O. P.; Zhu, Y.; Kairemo, K. Targeted Liposomal Drug Delivery in Cancer. *Curr. Pharm. Des.* **2004**, *10*, 2981–2989.

22. Flenniken, M.; Uchida, M.; Liepold, L.; Kang, S.; Young, M.; Douglas, T. A Library of Protein Cage Architectures as Nanomaterials. *Curr. Top. Microbiol. Immunol.* **2009**, *327*, 71–94.

23. Tong, G. J.; Hsiao, S. C.; Carrico, Z. M.; Francis, M. B. Viral Capsid DNA Aptamer Conjugates as Multivalent Cell-Targeting Vehicles. *J. Am. Chem. Soc.* **2009**, *131*, 11174–11178.

24. Wu, W.; Hsiao, S. C.; Carrico, Z. M.; Francis, M. B. Genome-Free Viral Capsids as Multivalent Carriers for Taxol Delivery. *Angew. Chem., Int. Ed.* **2009**, *48*, 9493–9497.

25. Valegrd, K.; Liljas, L.; Fridborg, K.; Unge, T. The Three-Dimensional Structure of the Bacterial Virus MS2. *Nature* **1990**, *345*, 36–41.

26. Xie, J.; Schultz, P. G. A Chemical Toolkit for Proteins—An Expanded Genetic Code. *Nat. Rev. Mol. Cell Biol.* **2006**, *7*, 775–782.

27. Mehl, R. A.; Anderson, J. C.; Santoro, S. W.; Wang, L.; Martin, A. B.; King, D. S.; Horn, D. M.; Schultz, P. G. Generation of a Bacterium with a 21 Amino Acid Genetic Code. *J. Am. Chem. Soc.* **2003**, *125*, 935–939.

28. Carrico, Z. M.; Romanini, D. W.; Mehl, R. A.; Francis, M. B. Oxidative Coupling of Peptides to a Virus Capsid Containing Unnatural Amino Acids. *Chem. Commun.* **2008**, 1205–1207.

29. Hooker, J. M.; Esser-Kahn, A. P.; Francis, M. B. Modification of Aniline Containing Proteins Using an Oxidative Coupling Strategy. *J. Am. Chem. Soc.* **2006**, *128*, 15558–15559.

30. Farokhzad, O. C.; Jon, S.; Khademhosseini, A.; Tran, T. T.; LaVan, D. A.; Langer, R. Nanoparticle−Aptamer Bioconjugates: A New Approach for Targeting Prostate Cancer Cells. *Cancer Res.* **2004**, *64*, 7668–7672.

31. Nimjee, S. M.; Rusconi, C. P.; Sullenger, B. A. Aptamers: An Emerging Class of Therapeutics. *Annu. Rev. Med.* **2005**, *56*, 555–583.

32. McNamara, J. O.; Andrechek, E. R.; Wang, Y.; Viles, K. D.; Rempel, R. E.; Gilboa, E.; Sullenger, B. A.; Giangrande, P. H. Cell Type-Specific Delivery of siRNAs with Aptamer-siRNA Chimeras. *Nat. Biotechnol.* **2006**, *24*, 1005–1015.

33. Bagalkot, V.; Farokhzad, O. C.; Langer, R.; Jon, S. An Aptamer-Doxorubicin Physical Conjugate as a Novel Targeted Drug-Delivery Platform. *Angew. Chem., Int. Ed.* **2006**, *45*, 8149.

34. Bagalkot, V.; Zhang, L.; Levy-Nissenbaum, E.; Jon, S.; Kantoff, P. W.; Langer, R.; Farokhzad, O. C. Quantum Dot-Aptamer Conjugates for Synchronous Cancer Imaging, Therapy, and Sensing of Drug Delivery Based on Bi-Fluorescence Resonance Energy Transfer. *Nano Lett.* **2007**, *7*, 3065–3070.

35. Chu, T. C.; Marks, J. W.; Lavery, L. A.; Faulkner, S.; Rosenblum, M. G.; Ellington, A. D.; Levy, M. Aptamer:Toxin Conjugates that Specifically Target Prostate Tumor Cells. *Cancer Res.* **2006**, *66*, 5989–5992.

36. Chu, T. C.; Twu, K. Y.; Ellington, A. D.; Levy, M. Aptamer Mediated siRNA Delivery. *Nucleic Acids Res.* **2006**, *34*, e73.

37. Hicke, B. J.; Stephens, A. W.; Gould, T.; Chang, Y.; Lynott, C. K.; Heil, J.; Borkowski, S.; Hilger, C.; Cook, G.; Warren, S.; Schmidt, P. G. Tumor Targeting by an Aptamer. *J. Nucl. Med.* **2006**, *47*, 668–678.

38. Bunka, D. H. J.; Stockley, P. G. Aptamers Come of Age—At Last. *Nat. Rev. Microbiol.* **2006**, *4*, 588–596.

39. Huang, Y.; Shangguan, D.; Liu, H.; Phillips, J. A.; Zhang, X.; Chen, Y.; Tan, W. Molecular Assembly of an Aptamer-Drug Conjugate for Targeted Drug Delivery to Tumor Cells. *ChemBioChem* **2009**, *10*, 862–868.

40. Ellington, A. D.; Szostak, J. W. *In Vitro* Selection of RNA Molecules That Bind Specific Ligands. *Nature* **1990**, *346*, 818–822.

41. Tuerk, C.; Gold, L. Systematic Evolution of Ligands by Exponential Enrichment: RNA Ligands to Bacteriophage T4 DNA Polymerase. *Science* **1990**, *249*, 505–510.

42. For crystal structure of aptamer shown in Figure 1, see: Huang, R.-H.; Fremont, D. H.; Diener, J. L.; Schaub, R. G.; Sadler, J. E. A Structural Explanation for the Antithrombotic Activity of ARC1172, a DNA Aptamer That Binds von Willebrand Factor Domain A1. *Structure* **2009**, *17*, 1476–1484.

43. Keefe, A. D.; Cload, S. T. SELEX with Modified Nucleotides. *Curr. Opin. Chem. Biol.* **2008**, *12*, 448–456.

44. Eulberg, D.; Klussmann, S. Spiegelmers: Biostable Aptamers. *ChemBioChem* **2003**, *4*, 979–983.

45. Shangguan, D.; Li, Y.; Tang, Z.; Cao, Z. C.; Chen, H. W.; Mallikaratchy, P.; Sefah, K.; Yang, C. J.; Tan, W. Aptamers Evolved from Live Cells As Effective Molecular Probes for Cancer Study. *Proc. Natl. Acad. Sci., U.S.A.* **2006**, *103*, 11838–11843.

46. Shangguan, D.; Tang, Z.; Mallikaratchy, P.; Xiao, Z.; Tan, W. Optimization and Modifications of Aptamers Selected from Live Cancer Cell Lines. *ChemBioChem* **2007**, *8*, 603–606.

47. Shangguan, D.; Cao, Z.; Meng, L.; Mallikaratchy, P.; Sefah, K.; Wang, H.; Li, Y.; Tan, W. Cell-Specific Aptamer Probes for Membrane Protein Elucidation in Cancer Cells. *J. Proteome Res.* **2008**, *7*, 2133–2139.

48. McDonald, I. J.; Doughery, T. J. Basic Principles of Photodynamic Therapy. *J. Porphyrins Phthalocyanines* **2001**, *5*, 105–129.

49. Dolmans, D.E.J.G.J.; Fukumura, D.; Jain, R. K. Photodynamic Therapy for Cancer. *Nat. Rev. Cancer* **2003**, *3*, 380–387.

50. Sternberg, E. D.; Dolphin, D. Porphyrin-Based Photosensitizers for Use in Photodynamic Therapy. *Tetrahedron* **1998**, *54*, 4151–4202.

51. Ali, H.; van Lier, J. E. Metal Complexes as Photo- and Radiosensitizers. *Chem. Rev.* **1999**, *99*, 2379–2450.

52. Suci, P. A.; Varpness, Z.; Gillitzer, E.; Douglas, T.; Young, M. Targeting and Photodynamic Killing of a Microbial Pathogen Using Protein Cage Architectures Functionalized with a Photosensitizer. *Langmuir* **2007**, *23*, 12280–12286.

53. Shieh, Y.-A.; Yang, S.-J.; Wei, M.-F.; Shieh, M.-J. Aptamer-Based Tumor-Targeted Drug Delivery for Photodynamic Therapy. *ACS Nano* **2010**, 1433–1442.

54. Regehly, M.; Greish, K.; Rancan, F.; Maeda, H.; Böhm, F.; Röder, B. Water-Soluble Polymer Conjugates of ZnPP for Photodynamic Tumor Therapy. *Bioconjugate Chem.* **2007**, *18*, 494–499.

55. Tremblay, J.; Dussault, S.; Viau, G.; Gad, F.; Boushira, M.; Bissonnette, R. Photodynamic Therapy with Toluidine Blue in Jurkat Cells: Cytotoxicity, Subcellular Localization, and Apoptosis Induction. *Photochem. Photobiol. Sci.* **2002**, *1*, 852–856.

56. Ke, M. S.; Xue, L.; Feyes, D. K.; Azizuddin, K.; Baron, E. D.; McCormick, T. S.; Mukhtar, H.; Panneerselvam, A.; Schluchter, M. D.; Cooper, K. D.; Oleinick, N. L.; Stevens, S. R.; *et al.* Apoptosis Mechanisms Related to the Increased Sensitivity of Jurkat T-cells *vs* A431 Epidermoid Cells to Photodynamic Therapy with the Phthalocyanine Pc 4. *Photochem. Photobiol.* **2008**, *84*, 407–414.

57. Kruper, W. J.; Chamberlin, T. A.; Kochanny, M. J. Regiospecific Aryl Nitration of *meso*-Substituted Tetraarylporphyrins: A Simple Route to Bifunctional Porphyrins. *J. Org. Chem.* **1989**, *54*, 2753–2756.

58. Endo, M.; Fujitsuka, M.; Majima, T. Porphyrin Light-Harvesting Arrays Constructed in the Recombinant Tobacco Mosaic Virus Scaffold. *Chem.—Eur. J.* **2007**, *13*, 8660–8666.

59. Chen, Y.; Parr, T.; Holmes, A. E.; Nakanishi, K. Porphyrinmaleimides: Towards Thiol Probes for Cysteine Residues in Proteins. *Bioconjugate Chem.* **2008**, *19*, 5–9.

60. Lindig, B. A.; Rodgers, M. A. J.; Schapp, A. P. Determination of the Lifetime of Singlet Oxygen in D_2O Using 9,10-Anthracenedipropionic Acid, a Water-Soluble Probe. *J. Am. Chem. Soc.* **1980**, *102*, 5590–5593.

61. Chen, X.; Kis, A.; Zettl, A.; Bertozzi, C. R. A Cell Nanoinjector Based on Carbon Nanotubes. *Proc. Natl. Acad. Sci., U.S.A.* **2007**, *104*, 8218–8222.

62. Hatz, S.; Poulsen, L.; Ogilby, P. R. Time-Resolved Singlet Oxygen Phosphorescence Measurements from Photosensitized Experiments in Single Cells: Effects of Oxygen Diffusion and Oxygen Concentration. *Photochem. Photobiol.* **2008**, *84*, 1284–1290.

63. Hsiao, S. C.; Shum, B. J.; Onoe, H.; Douglas, E. S.; Gartner, Z. J.; Mathies, R. A.; Bertozzi, C. R.; Francis, M. B. Direct Cell Surface Modification with DNA for the Capture of Primary Cells and the Investigation of Myotube Formation on Defined Patterns. *Langmuir* **2009**, *25*, 6985–6991.

64. Fonseca, A. M.; Porto, G.; Uchida, K.; Arosa, F. A. Red Blood Cells Inhibit Activation-Induced Cell Death and Oxidative Stress in Human Peripheral Blood T Lymphocytes. *Blood* **2001**, *97*, 3152–3160.